HHS Public Access

Author manuscript

Anesthesiology. Author manuscript; available in PMC 2024 July 01.

Published in final edited form as:

Anesthesiology. 2023 July 01; 139(1): 49–62. doi:10.1097/ALN.0000000000004579.

Measures of information content during anesthesia and emergence in the *C. elegans* nervous system

Andrew S Chang, MS,
Boston University School of Medicine, Department of Physiology and Biophysics, Boston University, Boston, MA, USA

Gregory S Wirak, PhD,
Department of Physiology and Biophysics, Boston University, Boston, MA, USA

Duan Li, PhD,
Research Assistant Professor, Center for Consciousness Science, Department of Anesthesiology, University of Michigan Medical School, Ann Arbor, MI, USA

Christopher V Gabel, PhD,
Associate Professor of Physiology & Biophysics, Boston University, Boston, MA, USA

Christopher W Connor, MD PhD
Associate Professor of Anesthesiology, Department of Anesthesiology, Peri-operative and Pain Medicine, Brigham and Women's Hospital, Boston, MA, USA; Adjunct Associate Professor of Biomedical Engineering, Physiology & Biophysics, Boston University, Boston, MA, USA

Abstract

Background—Suppression of behavioral and physical responses defines the anesthetized state. This is accompanied, in humans, by characteristic changes in EEG patterns. However, these measures reveal little about the neuron or circuit-level physiological action of anesthetics, nor how information is trafficked between neurons. We assess whether entropy-based metrics can differentiate between the awake and anesthetized state in *C. elegans* and characterize emergence from anesthesia at the level of interneuronal communication.

Methods—Performing volumetric fluorescence imaging, we measure neuronal activity across a large portion of the *C. elegans* nervous system at cellular resolution during distinct states of isoflurane anesthesia as well as during emergence from the anesthetized state. Using a generalized

Corresponding Author: Dr. Christopher W Connor, Department of Anesthesiology, Perioperative and Pain Medicine, Brigham and Women's Hospital, 75 Francis Street, CWN L1, Boston, MA 02115, cconnor@bwh.harvard.edu.

Prior Presentations
Presented in part at the 2021 annual meetings of the AUA and IARS as Connor CW, Wirak GS, Chang AS, Gabel CV, "State decoupling of the *C. elegans* neural system under anesthesia and during emergence.", May 13-16 2021. Held virtually.
Presented in part at the CeNeuro 2022 conference as Chang AS, Gabel CV, Connor CW, "Evolution of neuronal activity and system entropy in *C. elegans* during emergence from isoflurane anesthesia.", July 24-27 2022, Vienna, Austria.

Conflicts of Interest
None.

Disclosures
Dr. Connor has consulted for Teleflex, LLC on issues regarding airway management and device design and for General Biophysics, LLC on issues regarding pharmacokinetics. These activities are unrelated to the material in this manuscript.
No other authors report disclosures.

model of interneuronal communication, we empirically derive new entropy metrics that can distinguish the awake and anesthetized states.

Results—We derive three new entropy-based metrics that distinguish between stable awake and anesthetized states (4% and 8% isoflurane, n=10) while possessing plausible physiological interpretations. State Decoupling is elevated in the anesthetized state(0%: 48.8±3.50%, 4%: 66.9±6.08%, 8%: 65.1±5.16%; 0% vs. 4%, P<0.001; 0% vs. 8%, P<0.001), while Internal Predictability (0%: 46.0±2.94%, 4%: 27.7±5.13%, 8%: 30.5±4.56%; 0% vs. 4%, P<0.001; 0% vs. 8%, P<0.001), and System Consistency (0%: 2.64±1.27%, 4%: 0.97±1.38%, 8%: 1.14±0.47%; 0% vs. 4%, P=0.006; 0% vs. 8%, P=0.015) are suppressed. These new metrics also resolve to baseline during gradual emergence of *C. elegans* from moderate levels of anesthesia to the awake state (n=8). We find that early emergence from isoflurane anesthesia in C. *elegans* is characterized by the rapid resolution of an elevation in high frequency activity (n=8, P=0.032). The entropy-based metrics Mutual Information and Transfer Entropy , however, did not differentiate well between awake and anesthetized states.

Conclusions—Novel empirically-derived entropy metrics better distinguish the awake and anesthetized states compared to extant metrics and reveal meaningful differences in information transfer characteristics between states.

Introduction

Information theoretic measures calculate how information is stored or shared in a system. If we conceptualize the nervous system as an information processing system, then it follows that these metrics can be applied to the investigation of neuronal dynamics and states. The roots of information theory were laid out in Claude Shannon's seminal 1948 paper "A Mathematical Theory of Communication".[1] Shannon established the system-agnostic paradigm for analyzing the transmission of information that now underpins all modern digital communications and machine learning,[2] and which has since been applied to investigate biological information encoding in neuroscience and anesthesia.[3–8] Shannon's conceptualization of "entropy" as a measure of the overall information content of a given signal has been particularly useful in the investigation of communication within nervous systems. Entropy measures the information content of an individual signal, but further metrics derive naturally to quantify the information transfer between two signals. Mutual Information quantifies the information content shared between two signals,[1] and Transfer Entropy measures the time-dependent transfer of information from one specified signal to another.[9]

General anesthesia is characterized by transitions between distinct brain states, as observed in humans by EEG[10,11] and functional magnetic resonance imaging,[12] and in model organisms such as *D. melanogaster*[13] and *C. elegans*[14,15]. Essentially all multicellular organisms are susceptible to exposure to volatile anesthetic agents at broadly similar concentrations.[16,17] However, it remains unclear how communication at a nervous system or local network level is altered by the mechanism of action at the neuron. The predominant hypothesis is that the behavioral endpoint results from a disruption in coordinated neural activity, thus causing dissociation between the organism and its stimuli.[11,15] Mutual Information and Transfer Entropy have been employed to investigate anesthetized

states,[3,4,7,8] but use of these existing metrics presupposes how information transfer is expected to change under anesthesia. We address this limitation using a novel generalized model of time-dependent information transfer and hypothesize that the application of this approach to multi-neuron activity recordings taken from *C. elegans* head ganglia[15,18] will discriminate between the awake and anesthetized states in the animal and furthermore characterize the recovery of the nervous system to the awake state.

Materials and Methods

C. elegans Strains

All experiments were on young adult hermaphrodites of the transgenic strain QW1217 (zfIs124[Prgef-1::GCaMP6s]; otIs355[Prab-3::NLS::tagRFP]). GCaMP6s, a fluorescent calcium reporter, and nuclear-localized RFP are both expressed pan-neuronally in this strain (gift of M. Alkema, University of Massachusetts, Worcester, Massachusetts). *C. elegans* were cultivated at 20°C on nematode growth medium seeded with E. coli OP50.

Imaging of Neuronal Activity

GCaMP6s and RFP fluorescence in the *C. elegans* head ganglia were captured in volumetric stacks using a Dual Inverted Selective Plane Illumination microscope (Applied Scientific Instrumentation, Eugene, OR) and water-immersed 0.8 NA 40× objective (Nikon, Melville, NY). GCaMP6s and RFP were respectively excited using 5mW 488nm and 561nm lasers (Vortan Laser Technology, Rocklin, CA). Volumes for each fluorescent channel (GCaMP6s and RFP) were obtained at rate of 2Hz. Animals were immobilized for imaging by encapsulation in a pad of permeable hydrogel consisting of 13.3% polyethylene glycol diacrylate (Advanced BioMatrix, Carlsbad, CA) with 0.1% Irgacure (Sigma-Aldrich, USA).[20] Hydrogel pads containing animals to be imaged were cured with ultraviolet light onto silanated glass coverslips, which were affixed to the bottom of 50mm Petri dishes with vacuum grease. Petri dishes were then filled with 50mL S-basal buffer (100mM NaCl, 50mM KPO4 buffer, 5μg/ml cholesterol) as the immersion medium. Tetramisole was added to this buffer at 5mM to further immobilize animals.

Extraction of Neuronal Activity

For each animal imaged, 120 neurons were tracked in the head region using the nuclear-localized RFP fluorophore, and their activity extracted using the fluctuations in cytoplasmic GCaMP6s neurofluorescence. This tracking and extraction procedure was performed as a massively parallel computation executed at the Massachusetts Green High Performance Computing Center using computational techniques as previously detailed in Awal et al. (2020).[15]

We make the assumption that the activity state of any given neuron can be approximated by the instantaneous calcium concentration in the soma of that neuron. However, the state-space of a neuron in a functioning network is certainly much more complex in truth, and limitations apply to the use of information theory in a system in which the state space of signals is incompletely observable. Calcium fluorescence does not report, for example, potentially relevant properties of the neuron under anesthesia such as the level of endocytic

activity.[21] Furthermore, it remains unknown if the state of a whole nervous system can be represented as the concatenation of the states of individual neurons within it. We make these base assumptions due to technical limitations and theoretical gaps in knowledge.

Regimes of Isoflurane Anesthesia in *C. elegans*

C. elegans become anesthetized on exposure to isoflurane with a MAC value of approximately 3% at room temperature.[14] At 17°C, isoflurane is 2.3 times more soluble in tissues such as muscle and fat than at 37°C,[22] and consequently absorption of a larger quantity of isoflurane is required to produce a similar chemical potential gradient at cooler temperatures. A concentration of 3% isoflurane at 17°C is thus pharmacodynamically similar, in respect of its physical chemistry, to a concentration of 1.3% at 37°C. Alterations in *C. elegans* neuronal activity in response to isoflurane exposure were assessed using two experimental regimes: stepwise anesthetization and emergence.

Stepwise Anesthetization—Three 5-minute-long neuronal activity recordings were taken from each animal (n=10) after progressive equilibration to 0%, 4%, and 8% atmospheric isoflurane.[14] These concentrations correspond to 1.3 and 2.6 MAC respectively, which are appropriate to obtain consistent moderate and deep anesthesia. Imaging was performed at time t = 30 min, 150 min, and 270 min from the start of the experiment at isoflurane levels of 0%, 4% and 8%. Isoflurane levels were stepped by exchanging the immersion medium for fresh S-basal buffer with the addition of 13 μl or 26 μl pipetted isoflurane for isoflurane 4% and 8% respectively. The atmosphere within the covered Petri dish was then equilibrated, during the time between imaging sequences, to a concentration of 4% or 8% respectively using continuous monitoring with an infra-red spectrometer (Ohmeda 5250 RGM, GE Healthcare, Madison, WI) and instillation of isoflurane via syringe pump as necessary to maintain the targeted concentration.

Emergence—While encapsulated and immersed in 50ml of S-basal buffer, *C. elegans* (n=8) were imaged for 10 minutes in a pre-anesthetized state (i.e. isoflurane 0%). 49ml of buffer was then withdrawn from the Petri dish and reserved, and each animal was equilibrated to an atmosphere of isoflurane 4% for 120 minutes as described above while immersed in 1ml of buffer. The Petri dish was then unsealed and the 49ml of buffer solution was reintroduced, thus immediately reducing the buffer concentration of isoflurane to 1/50th of its previous level. A 120-minute-long neuronal activity recording was initiated immediately after the dilution of buffer, capturing each animal's emergence from the anesthetized state. Controls (n=8) were performed by resting animals in room air for 120 minutes before commencement of post-dilution activity recording.

Statistical Methods

Normalization of neuronal activity traces—In recordings from the stepwise equilibration regime, neuronal activity intensity for all three recordings in each animal (0%, 4%, and 8%) was normalized against the average intensity across all neurons and time points in the 0% isoflurane recording. In recordings from the emergence regime, neuronal activity intensity in each recording was normalized to the average intensity across all neurons and time points in that recording. Because the animals are immobilized and encapsulated in a

hydrogel for imaging, it is not possible to normalize to an alternative behavioral endpoint such as wakefulness.

Signal power and spectral density analysis—Signal power was calculated for each neuronal trace in each animal in the stepwise equilibration experimental regime and averaged by exposure condition (0%, 4%, and 8 isoflurane). Means were compared with one-way ANOVA and the two-tailed independent samples t-test. The time differential for each neuronal trace in each 120-minute-long emergence recording was calculated using total-variation regularization,[23] and the power spectral density was calculated over sequential 12-minute epochs by Fourier transformation. Power spectra were averaged across all 120 neurons tracked in each animal to produce a mean power spectrum for each animal at each epoch, with cumulative power spectra and median power frequencies calculated from these mean power spectra. Differences in mean spectral median frequencies between animals emerging from 4% isoflurane exposure and control animals were compared using the two-tailed independent samples t-test.

Statistical significance was defined at $P<0.05$, with further highlighting of results demonstrating $P<0.01$ and $P<0.001$ respectively. A formal *a priori* power calculation for the number of experimental animals was not performed; previous experience with this animal model indicated that the number used here would be sufficient to detect significant changes.[14,15] Data analysis was performed using Matlab (MathWorks, Natick, MA).

Entropy Calculations and Derived Metrics

Entropy can be intuited as a measure of the “amount of information” present in a given signal. It can be calculated for any signal that consists of a series of discrete states. It is maximized when that signal is maximally disordered, i.e. when all possible discrete states within the signal occur with equal probability. Entropy can also be interpreted as quantifying the level of surprise or unpredictability in a signal. Given multiple signals, the joint entropy reflects the combined entropy of those signals. Mutual Information, as introduced by Shannon and later named by Fano,[1,24] represents the mutual dependence of two (or more) signals. Mutual Information can also be understood as the amount of information provided by one signal about another, a formulation that is frequently applied to the quantification and modeling of coherence between neural signals, from unit spiking to EEG.[3–6]. The basic mathematical details of entropy, joint entropy and Mutual Information are reviewed in Appendix A, accompanied by a valuable and extensible graphical analogy.

Transfer Entropy is inherently directional and time-dependent. For a system consisting of two signals X and Y, the transfer entropy from X to Y ($TE_{X\rightarrow Y}$) represents the amount of information shared between the past of X and the future of Y that is not shared with the past of Y. It is therefore a measure of the extent to which the past of X causes the future of Y. This dependence on time requires separating each source into past and future, and thus the two-signal system of X and Y becomes are four-signal system consisting of X_P, X_F (the past and future of X) and Y_P, Y_F (the past and future of Y).[9] The relationship between the information content in this four-signal model consisting of X_P, Y_P, X_F and Y_F can be illustrated as the intersections of a 4-set Venn diagram (Figure 1A) comprising 15

discrete numbered regions. The Mutual Information between the pasts of X and Y is as shown in Figure 1B; the sum of the information in regions 3, 7, 11, and 15. The transfer entropy from signal X to signal Y, $TE_{X\rightarrow Y}$, can then be understood as the intersection of $\mathbf{X_P}$ with the intersection of $\mathbf{Y_F}$ and the complement of $\mathbf{Y_P}$ (Figure 1C): the information in the past of X shared with the future of Y that is not shared with the past of Y itself, and hence the sum of the information in regions 9 and 13. A rigorous formal algebra connects these equivalent entropy and set representations.[25] For simplicity, Table 1 shows the full conversion between each set region and the joint entropies of X_P, Y_P, X_F and Y_F. Thus, the amount of information in region 1 (i.e. the amount of information in X_P that is not shared with any of Y_P, X_F and Y_F) is given by $H(X_P, X_F, Y_P, Y_F) - H(X_F, Y_P, Y_F)$. $TE_{X\rightarrow Y}$, given by the sum of regions 9 and 13, is $H(X_P, Y_P) + H(Y_P, Y_F) - H(X_P, Y_P, Y_F) - H(Y_P)$. Once illustrated graphically, it becomes obvious that we are not limited to pre-existing metrics such as Mutual Information or TE, but that we may select any additive combination of the 15 regions of the four-signal model between neuron pairs in the awake and anesthetized states that we choose. Thus, we can empirically construct new metrics that have the potential to better characterize how neuron-to-neuron information transfer is altered in the anesthetized state, whose physiological rationale can be made explicit. The null hypothesis is that there should be no significant difference seen in entropy measurements at different levels of anesthesia. By extension, the null hypothesis is also that no grouping of entropy calculations (e.g. MI, TE) should differ significantly across different levels of anesthesia.

The four-signal model in C. elegans during stable levels of anesthesia.—The four-signal model requires that the continuous traces of *C. elegans* neuronal activity data be discretized into a set number of quantized activity states. The GCaMP fluorescence data was quantized to four levels using optimum thresholds derived using Otsu's Algorithm, thus producing a 2-bit value for each neuron at each imaging time step for each animal.[26,27]. The same thresholds were used across all states (isoflurane 0%, 4%, 8%), on a per animal basis. The thresholds were recalculated using Otsu's Algorithm for each individual animal, which compensates for such issues as experimental variability in fluorophore expression between animals or strength of illumination. This quantization scheme was chosen due to previous success with this approach.[14] Sources X and Y are any pair of neurons drawn from the pool of 120 neurons whose activity was extracted, thus generating 14400 neuron-pairs, with X_P, Y_P, X_F and Y_F generated by time-shifting by 1 second (i.e. by 2 samples). This 4-signal model can assess the tendency for a neuronal signal (i.e. X_P) to predict the next one-second of either that same signal (X_F) or the next one-second of another neuron's signal (Y_F). Entropy content was also normalized by the joint entropy $H(X_P, X_F, Y_P, Y_F)$, which corresponds to the sum of all 15 regions or $\mathbf{X_P} \cup \mathbf{X_F} \cup \mathbf{Y_P} \cup \mathbf{Y_F}$; this allows the proportional distribution of entropy to be analyzed independently of changes in total entropy across treatment conditions. We compared the entropy distributions of MI, TE, and new empirically-defined metrics by pooling the entropy content of all possible neuron pairs in each animal by treatment condition and comparing the mean entropy content in each information region across conditions with ANOVA, with multiple comparisons performed with a Tukey-Kramer adjustment.

The four-signal model in C. elegans during emergence.—Mutual Information, Transfer Entropy and other new metrics were calculated as above but under a moving window of ± 2 minutes (i.e. ± 240 samples) across the 120 minutes of emergence neuronal activity data. Average time courses were time-smoothed using a moving mean operator with a 100 second window to better reveal the trend of the data while suppressing superimposed periodic variations, and 95% confidence intervals were calculated for averaged time courses.

Results

Isoflurane exposure suppresses power and the total entropy of neuronal activity

Figures 2Aabc show examples of the gross alterations in neuronal activity that accompany anesthesia with isoflurane at 0 MAC, 1.3 MAC and 2.6 MAC (isoflurane 0%, 4%, 8% respectively). The mean signal power in anesthetized animals decreases compared to unanesthetized animals (Figure 2Ad). After discretization, the total entropy also reduces with increasing isoflurane levels (Figure 2Ae). The lower activation level of the neurons overall results in a smaller number of accessible neurological states and consequently a lower total entropy.

A resolving high-frequency spectral shift characterizes early emergence from isoflurane

Isoflurane exposure at 4% in *C. elegans* has previously been demonstrated to cause a shift in the mean spectral power of neuronal activity towards higher frequencies. This effect is grossly visible in Figure 2Ab: when compared to the activity at 0% in Figures 2Aa and 2Ba, the activity at 4% appears less settled and more jittery even though the total signal power and entropy are lower. This behavior appears to characterize the general shift from ordered activation and deactivation of suites of networked neurons in the baseline unanesthetized state towards less organized and rapidly shifting dynamics in the isoflurane induced anesthetized state.[15] Figure 2Bb shows the progressive resolution of this neuronal activity in emerging from isoflurane 4% to 0%. At 0.2 hours, we find that high-frequency content is greatly enriched after exposure to isoflurane 4% compared to controls. However, this phenomenon resolves quickly during anesthesia emergence, and the power spectra of emerging and control animals do not appear different by 0.8 hours (Figure 2Bc). This result is further quantified by measuring the median power frequency during each 0.2 hour epoch during emergence (n=8 emerging from isoflurane 4%, n=8 controls). The median power frequency in *C. elegans* exposed to isoflurane 4% was significantly elevated compared to control animals at 0.2 hours post-exposure (Figure 2Bd, two-tailed independent samples t-test, P=0.032) with no significant differences between treatment groups observed beyond that time point .

Exposure to isoflurane significantly alters the distribution of entropy

The proportional entropy content in each information region was averaged across all neuron pairs across all animals within each isoflurane exposure level (0%, 4%, 8%) as shown in Figure 3, with the numbering and coloring of regions consistent with Figure 1A. For comparison, Supplemental Figure S1A shows the absolute distribution of entropy content across these regions (which also reflects the decline in overall entropy seen with deeper levels of anesthesia seen in Figure 2Ae), and Supplemental Figure S1B shows the

proportional distribution of entropy under an alternative encoding strategy that places greater emphasis on the time-course of neuron activity at the expense a cruder quantization of the level of activity into fewer bins.

Isoflurane exposure at 4% and 8% in *C. elegans* is associated with significantly elevated proportional entropy in regions 1, 2, 4, and 8, representing the quantity of information contained in each of the respective signals in the four-signal model (X_P, Y_P, X_F, Y_F) that is not shared with any of the other three signals. Proportional entropy content is also significant reduced in regions 5 and 10 under anesthesia, representing the amount of information in a neuron's past state (X_P or Y_P) that is predictive of its future state (X_F or Y_F, respectively) that is independent of information present in another neuron (Y or X, respectively). Finally, we observe that the proportional content in region 15 is also lower under anesthesia; this region is intuitively the information shared among all four signals, $\mathbf{X_P} \cap \mathbf{X_F} \cap \mathbf{Y_P} \cap \mathbf{Y_F}$.

From these results, we can empirically construct and name new metrics by grouping those information regions observed to exhibit altered entropy content in anesthetized animals and which, when so grouped, are conceptually meaningful regarding how information transfer could be altered in the anesthetized state. Three such metrics are:

- **State Decoupling.** The sum of regions 1, 2, 4 and 8 describes the amount of information present in only one of the signals X_P, Y_P, X_F, Y_F and hence the extent to which neurons become decoupled from each other and from themselves.
- **Internal Predictability.** The sum of regions 5 and 10 describes the extent to which the past state of a neuron is predictive of its future behavior, independent of other sources of information.
- **System Consistency.** Region 15 alone represents that amount of state information that is present in both the past and future of both sources X and Y, and hence the extent to which the system remains in a mechanistically consistent condition. This metric is similar to a system-wide expansion of the concept of multiinformation, as previously measured within the circumscribed and well-defined group of neurons that comprise the *C. elegans* motor circuit.[14]

Pre-existing metrics poorly distinguish the awake versus the anesthetized state

Mutual Information and Transfer Entropy are represented graphically in Figures 4Aa and 4Ba respectively. These metrics were calculated across all possible functional neuron pairs in the cohorts of animals exposed to stepwise equilibrated 0%, 4%, and 8% isoflurane (n=10). No statistically significant difference is seen in Mutual Information between anesthetized states and the control state (Figure 4Ab, 0% isoflurane: 3.67 ± 1.35%, 4% isoflurane: 2.26 ± 1.71%, 8% isoflurane: 2.29 ± 0.83%; ANOVA, P=0.043; Tukey-Kramer 0% vs 4%; P=0.069, Tukey-Kramer 0% vs 8%, P=0.075). Transfer entropy was found to be elevated in the 4% isoflurane-exposed state relative to controls (Figure 4Bb, 0% isoflurane: 0.58 ± 0.08%, 4% isoflurane: 0.98 ± 0.27%, 8% isoflurane: 0.71 ± 0.34%; ANOVA, P=0.004; Tukey-Kramer 0% vs 4%, P=0.004; Tukey-Kramer 0% vs 8%, P=0.483), but not in the 8% isoflurane-exposed state.

In comparison, Figures 4CDE show the graphical representation and entropy formulae for State Decoupling, Internal Predictability and System Consistency, as well as the effect of isoflurane anesthesia upon these new metrics. State Decoupling is elevated in both the 4% and 8% isoflurane exposure groups relative to controls with a high degree of significance (Figure 4Cb, 0% isoflurane: 48.8 ± 3.50%, 4% isoflurane: 66.9 ± 6.08%, 8% isoflurane: 65.1 ± 5.16%; ANOVA, $P<0.001$; Tukey-Kramer 0% vs 4%, $P<0.001$; Tukey-Kramer 0% vs 8%, $P<0.001$), whereas the Internal Predictability is suppressed in both the 4% and 8% isoflurane cohorts relative to control with a high degree of significance (Fig. 4Db, 0% isoflurane: 46.0 ± 2.94%, 4% isoflurane: 27.7 ± 5.13%, 8% isoflurane: 30.5 ± 4.56%; ANOVA, $P<0.001$; Tukey-Kramer 0% vs 4%, $P<0.001$; Tukey-Kramer 0% vs 8%, $P<0.001$). The metric of System Consistency (as a generalization of multiinformation) is also significantly suppressed under 4% and 8% isoflurane exposure relative to controls (Fig. 4Eb, ANOVA, 0% isoflurane: 2.64 ± 1.27%, 4% isoflurane: 0.97 ± 1.38%, 8% isoflurane: 1.14 ± 0.47%; $P=0.004$; Tukey-Kramer 0% vs 4%, $P=0.006$; Tukey-Kramer 0% vs 8%, $P=0.015$).

Emergence from isoflurane anesthesia is well-characterized by novel entropy-based metrics

Mutual Information, Transfer Entropy, State Decoupling, Internal Predictability, and System Consistency were calculated for all possible functional neuron pairs under a moving window across a 120 minute emergence period (n=8 emerging from isoflurane 4%, n=8 controls). The average values for these metrics were then calculated as smoothed means with 95% confidence intervals over the emergence period as shown in Figure 5 for each metric respectively (isoflurane 4% emergence in the purple band, controls in the grey band). We observe that the degree of separation in each metric between then isoflurane 4% and control conditions compares well with equivalent measurements at stable levels of anesthesia, as reported above. The separation of the means resolves over the imaging period for all five assessed metrics. However, the separation of means for Mutual Information and Transfer Entropy (Figures 5A and 5B) is small, and any difference resolves relatively early in the emergence timeline. The novel metrics of State Decoupling (Figure 5C) and Internal Predictability (Figure 5D) demonstrate very distinct separation of means between the anesthetized and control conditions with resolution of these differences appearing much later in the emergence timeline, more than an hour after beginning emergence from anesthesia. The System Consistency (Figure 5E) begins with a smaller, though clear, separation of means and appears to resolve along a timeline most consistent with that seen for the more classical measurement of Median Power Frequency as shown in Figure 2Bd.

A slow drift is seen in the smoothed means of control animals across all metrics. This is most likely a technical artifact, arising from a combination of progressive photobleaching of the GCaMP fluorophores under prolonged imaging coupled with a tendency towards diminishing sensory input and more quiescent neuronal activity in *C. elegans* specimens that are encapsulated and immobile. The relevant findings are the resolution of the differences between the isoflurane and control populations.

Entropy-based measures resolve non-linearly as animals emerge from isoflurane anesthesia

Although the bands of the means of the metrics in Figure 5 are smooth, there are considerable periodic fluctuations in the underlying signals of the individual experimental animals, both in the isoflurane and control cohorts, over short time scales. The trends reliably resolve over the emergence period imaged, but this appears to occur non-linearly with regard to the underlying individual metrics. Indeed, the non-linearity of emergence is evident by visual inspection of the neuronal traces displayed in the example trial, Figure 2Bb, where the animal clearly passes through periods of relative neuronal quiescence and higher neuronal activity over the two hours of the recording.

Discussion

We applied a generalized model of neuron-to-neuron information transfer to construct novel entropy metrics beyond the standard forms of Mutual Information and Transfer Entropy. Mutual Information and Transfer Entropy fared poorly in distinguishing awake and anesthetized states in C. *elegans* under isoflurane anesthesia. Rather than rely on preconceptions about how anesthesia affects neuron-to-neuron information transfer, our approach allows for conceptualization of new metrics based on empirical measurements. These new metrics, named State Decoupling, Internal Predictability and System Consistency, better differentiate the awake state from isoflurane anesthetized states in *C. elegans*.

What can this tell us about how neuron-to-neuron communication is altered during anesthesia? The increase in state decoupling in anesthetized animals plausibly describes individual neurons becoming decoupled from their previous state and the state of surrounding neurons, representative of an induced disorder of the usual functioning of the neurological system at the level of neuron-to-neuron communication. This result corresponds well with observations across species that the anesthetized state is associated with apparent informational decoupling. Similarly, the decrease in system consistency between neurons in anesthetized animals can be interpreted as the inverse effect; as the nervous system becomes anesthetized, the amount of information shared between neurons decreases, and the overall predictability of neuronal activity, even by any given neuron's own past activity, is also reduced.[13–15,19,28] This latter effect is captured by a reduction in the metric of internal predictability in the anesthetized state. There is necessarily some concordance between the physiological interpretations of these new metrics. A gain of relative entropy content in one information region must be made up for by the loss of relative entropy content in others. The elevation of relative entropy content in the information regions defining State Decoupling is balanced by the loss of relative entropy content in the regions defining Internal Predictability and System Consistency. Our grouping of certain information regions into particular metrics is a method for expressing and interpreting an overall shift in the shape of entropy content distribution between the awake and anesthetized states. The broader utility of the specific metrics we have defined in this study to explain neuronal dysfunction requires further investigation in other systems.

One important consideration is whether these effects are simply due to an overall reduction in the information content of individual neurons as the animal becomes more deeply anesthetized. Indeed, we do observe that the mean entropy of individual neuronal activity signals in *C. elegans* significantly decreases in a dose-dependent fashion after exposure to isoflurane, accompanied by a suppression of overall activity. However, all entropy-based metrics calculated were normalized to the total joint entropy of the four-signal model used to generate them. Consequently, we demonstrate that changes in overall entropy content in the system cannot account for observed alterations in the normalized entropy content of information regions or any derivative metrics. Rather, changes in our entropy-based metrics reflect changes in the distribution of entropy among different information regions, and therefore alterations in how the information content of each neuronal pair is communicated. We find it fundamentally interesting that our entropy-based metrics strongly distinguish between the awake and anesthetized states in a seemingly binary fashion, while metrics assessing the mean behavior of individual neurons, such as mean entropy and mean signal power change in a graded fashion as the animal is exposed greater levels of anesthesia. The differential sensitivity of these metrics suggests that breakdown in neuron-to-neuron communication in the anesthetized state is not merely a linear function of global suppression of neuronal activity.

Transfer Entropy was significantly elevated in *C. elegans* at equilibration to isoflurane 4% but not in those equilibrated to isoflurane 8% when compared to controls. How does this paradoxical result arise? Transfer Entropy measures the extent to which the future of a source (e.g. Y_F) is influenced by the past of another source (e.g. X_P) but not by its own past (e.g. Y_P). If there is an increase in high frequency activity and instability in Y (i.e., less internal predictability in Y) then the past of X can have proportionally more influence on future Y than Y's own past. Hence, Transfer Entropy can be elevated at isoflurane 4%. Transfer Entropy may be lower when there is greater regularity in the nervous system as at isoflurane 0%, or when neuronal activity becomes comparatively static as at isoflurane 8%.

A limitation of this current study is that neurons are not individually identified. One of the strengths of C. *elegans* as a model system is the ability to leverage the availability of a comprehensive neuronal connectome[29] and genetic fate mapping data,[30–32] making neuronal identification a potentially very powerful approach. Indeed, we previously applied entropy to the analysis of a circuit of five manually identified neurons (AVA, AVB, AVD, AVE, RIM).[14] Recent advances in the polychromatic labeling of C. *elegans* neurons bring automated neuronal identification at scale to the cusp of practicability.[33] Neuronal identification allows for comparison of specific neuron pairs across subjects, precisely identifying information transfer between neurons that are known to be mechanistically linked or alternately allowing for segmentation the neuronal population based on activity.[15] In the future, we anticipate that it will become possible to reconcile specific neuronal behaviors under anesthesia to chemical and electrical synaptic density as established by neuronal identification and the connectome..[14] During deep anesthesia, neuronal dynamics become relatively static with neurons apparently locked into specific levels of activation. Does this represent a freezing of state in some moment of anesthesia, or is this pattern reproduced across individuals based upon the action of isoflurane on the underlying fixed

connectome?[29] Neuronal identification will clarify which of these plausible hypotheses is true. This would fundamentally influence our understanding of the mechanism of action.

Neuronal identification would also allow us to further probe the non-linear nature of anesthetic emergence including what appears to be periods of global neuronal quiescence. We demonstrate that the anesthetized state and early emergence is characterized by an elevation in high frequency activity. However, once this effect abates, what remains appears to be periods of suppressed neuronal activity sporadically interspersed with periods of activity. This pattern is evident in Figure 2Bb; it is present in almost all 4% isoflurane emergence trials but is not present in any control trials. Likewise, we note significant short-term oscillations in the entropy-based metrics of individual trials displayed in Figure 5. C. *elegans* is known to enter periods of lethargus, a physiologic sleep-like state characterized by a lack of physical movement and global neuronal quiescence.[34] The periods of broad neuronal quiescence we observe here appear similar to the neuronal activity patterns in C. *elegans* lethargus, suggesting the animal may be passing in and out of a “sleep-like” state after isoflurane emergence. In the future, neuronal identification within the C. *elegans* imaging assays will allow us to probe this hypothesis further as we will identify and measure the activity of specific sleep-associated neurons, such as the interneuron RIS, in anesthetized and emerging animals.

Work in human subjects has been largely based on studies analyzing EEG and functional magnetic resonance imaging data in anesthetized volunteers, although these approaches can only address the question of communication in the nervous system on a region-to-region basis rather than a neuron-to-neuron basis.[35–38] Our work applies an information theoretic approach to anesthesia at a more exquisite scale, but our findings are broadly consistent with a network inefficiency conceptualization of anesthesia. Network disruption between cortical “nodes” may well be an emergent outcome of network disruption at the subcortical level. We observed, during the emergence trials, that entropy metrics are strikingly non-smooth in both control and anesthetized animals alike even though stable trends are produced. Neuron-to-neuron information transfer is natively in a state of rapid flux. This finding is particularly interesting in light of studies demonstrating a rhythmic oscillation between brain states, as measured by local field potential and EEG, in animals exposed to steady-state concentrations of anesthetics.[39–41] It is known that C. *elegans* has transient metastable states that encode specific gross behaviors, and that C. *elegans* transitions between these states as it performs these different behaviors.[42] We previously reproduced these state-space findings in awake worms and demonstrated that under isoflurane anesthesia the ability to form these representative metastable states is lost.[15] Our findings lend further credence to approaching emergence from anesthesia to wakefulness as a stochastic process,[43] in which the probability of the nervous system being in activity states associated with wakefulness versus sedation increases over time.

Recent investigations on the internal operation of the clinical BIS monitor have revealed algorithms that it applies to the frontal EEG.[44] While the BIS monitor does not explicitly calculate entropy, an algorithm that it most commonly applies under general anesthesia can be effectively restated in terms of the Wiener Entropy across the low gamma EEG band (40 – 47 Hz) relative to the Wiener Entropy across the whole power spectrum (0 – 47

Hz).[45] It makes sense that information theory should remain an appropriate tool to assess the effects of anesthetics even over the enormous scale difference between the *C. elegans* nervous system and the primate brain.

Supplementary Material

Refer to Web version on PubMed Central for supplementary material.

Financial Support

NIH R35 GM145319

NIH R01 GM121457

Departmental support

Appendix A

Given a signal source X, the entropy H(X) represents the information content of that signal. Assuming that X can be in a finite number of states [x_1, x_2, x_3, …, x_n] with probabilities [P(x_1), P(x_2), P(x_3), …, P(x_n)], then the information content is given by the Shannon entropy function:

$$H(X) = -\sum_{i=1}^{n} P(x_i)\log_2 P(x_i) \quad \text{(Eq A1)}$$

where H(X) is in *bits* if the logarithm is base-2. The entropy is maximal when the states x_i are all equally probable, and the entropy drops to zero if any one state is certain. If a process involves two signal sources, X and Y, then it is natural to question what information is contained in both sources and whether any information is shared between the two. Assuming X and Y have states x and y respectively, the entropy of both sources together (i.e. the joint entropy) is:

$$H(X,Y) = -\sum_{x \in X}\sum_{y \in Y} P(x,y)\log_2 P(x,y) \quad \text{(Eq A2)}$$

and the Mutual Information (MI), denoted as I(X;Y), which is the information that is common to both sources is given by:

$$I(X;Y) = -\sum_{x \in X}\sum_{y \in Y} P(x,y)\log_2 \frac{P(x,y)}{P(x)P(y)} \quad \text{(Eq A3)}$$

When both sources X and Y are independent of each other, the mutual information is zero.

Such equations are challenging to manipulate and conceptualize, and so it is helpful to note that it is possible to rewrite Equation A3 as a simple combination of the underlying entropies:

$$I(X;Y) = H(X) + H(Y) - H(X, Y) \quad \text{(Eq A4)}$$

Problems in the amount of information, as described above, have a dual relationship based in additive set functions.[24] This dual relationship can be considerably more intuitive. The idea is rather like the equivalence between the time-domain and frequency-domain of a signal: although these representations are equivalent, some problems are easier to solve in one domain than the other, and thus it is often useful to convert between the two domains. For example, if **X** and **Y** represent the corresponding sets for sources X and Y, then the mutual information I(X;Y) shared between the sources X and Y is simply $\mathbf{X} \cap \mathbf{Y}$, and the joint entropy is $\mathbf{X} \cup \mathbf{Y}$. Hence:

$$\mathbf{X} \cap \mathbf{Y} = \mathbf{X} + \mathbf{Y} - \mathbf{X} \cup \mathbf{Y} \quad \text{(Eq A5)}$$

Consequently, in its dual representation as an additive function of sets, the mutual information (MI) shared between X and Y can be immediately visualized and calculated as:

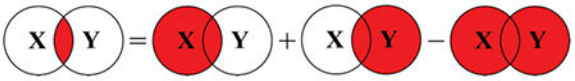

(Eq A6)

Equations A3 and A6 are equivalent representations, yet the graphical form of Equation A6 is significantly more intuitive to manipulate and more useful for constructive reasoning.

References

1. Shannon CE: A mathematical theory of communication. The Bell System Technical Journal 1948; 27: 379–423
2. Connor CW: Artificial Intelligence and Machine Learning in Anesthesiology. Anesthesiology 2019; 131: 1346–1359 [PubMed: 30973516]
3. Hudetz AG, Pillay S, Wang S, Lee H: Desflurane Anesthesia Alters Cortical Layer–specific Hierarchical Interactions in Rat Cerebral Cortex. Anesthesiology 2020; 132: 1080–1090 [PubMed: 32101967]
4. Lipping T, Saareleht J, Olejarczyk E, Sonkajärvi E, Ylinen T, Jäntti V: Synchronization of brain activity during induction of propofol anesthesia: Comparison of methods, 38th Annual International Conference of the IEEE Engineering in Medicine and Biology Society, 2016, pp 5505–5508
5. Prince LY, Tran MM, Grey D, Saad L, Chasiotis H, Kwag J, Kohl MM, Richards BA: Neocortical inhibitory interneuron subtypes are differentially attuned to synchrony- and rate-coded information. Communications Biology 2021; 4: 935 [PubMed: 34354206]
6. Roy A, Narayanan R: Spatial information transfer in hippocampal place cells depends on trial-to-trial variability, symmetry of place-field firing, and biophysical heterogeneities. Neural networks : the official journal of the International Neural Network Society 2021; 142: 636–660 [PubMed: 34399375]
7. Wollstadt P, Sellers KK, Hutt A, Frohlich F, Wibral M: Anesthesia-related changes in information transfer may be caused by reduction in local information generation, 2015 37th Annual International

Conference of the IEEE Engineering in Medicine and Biology Society (EMBC), 2015, pp 4045–4048

8. Wollstadt P, Sellers KK, Rudelt L, Priesemann V, Hutt A, Fröhlich F, Wibral M: Breakdown of local information processing may underlie isoflurane anesthesia effects. PLOS Computational Biology 2017; 13: e1005511 [PubMed: 28570661]
9. Schreiber T: Measuring Information Transfer. Physical Review Letters 2000; 85: 461–464 [PubMed: 10991308]
10. Brown EN, Purdon PL, Van Dort CJ: General Anesthesia and Altered States of Arousal: A Systems Neuroscience Analysis. Annual Review of Neuroscience 2011; 34: 601–628
11. Kelz MB, Mashour GA: The Biology of General Anesthesia from Paramecium to Primate. Current Biology 2019; 29: R1199–R1210 [PubMed: 31743680]
12. Ranft A, Golkowski D, Kiel T, Riedl V, Kohl P, Rohrer G, Pientka J, Berger S, Thul A, Maurer M, Preibisch C, Zimmer C, Mashour GA, Kochs EF, Jordan D, Ilg R: Neural Correlates of Sevoflurane-induced Unconsciousness Identified by Simultaneous Functional Magnetic Resonance Imaging and Electroencephalography. Anesthesiology 2016; 125: 861–872 [PubMed: 27617689]
13. van Swinderen B: A succession of anesthetic endpoints in the Drosophila brain. Journal of Neurobiology 2006; 66: 1195–1211 [PubMed: 16858694]
14. Awal MR, Austin D, Florman J, Alkema M, Gabel CV, Connor CW: Breakdown of Neural Function under Isoflurane Anesthesia: In Vivo, Multineuronal Imaging in Caenorhabditis elegans. Anesthesiology 2018; 129: 733–743 [PubMed: 30004907]
15. Awal MR, Wirak GS, Gabel CV, Connor CW: Collapse of Global Neuronal States in Caenorhabditis elegans under Isoflurane Anesthesia. Anesthesiology 2020; 133: 133–144 [PubMed: 32282426]
16. Crowder CM: Does natural selection explain the universal response of metazoans to volatile anesthetics? Anesth Analg 2008; 107: 862–3 [PubMed: 18713896]
17. Eckenhoff RG: Why can all of biology be anesthetized? Anesth Analg 2008; 107: 859–61 [PubMed: 18713895]
18. Wirak GS, Florman J, Alkema MJ, Connor CW, Gabel CV: Age-associated changes to neuronal dynamics involve a disruption of excitatory/inhibitory balance in C. elegans. Elife 2022; 11: e72135 [PubMed: 35703498]
19. Mashour GA: Network Inefficiency: A Rosetta Stone for the Mechanism of Anesthetic-induced Unconsciousness. Anesthesiology 2017; 126: 366–368 [PubMed: 28092319]
20. Burnett K, Edsinger E, Albrecht DR: Rapid and gentle hydrogel encapsulation of living organisms enables long-term microscopy over multiple hours. Communications Biology 2018; 1: 1–10 [PubMed: 29809203]
21. Jung S, Zimin PI, Woods CB, Kayser EB, Haddad D, Reczek CR, Nakamura K, Ramirez JM, Sedensky MM, Morgan PG: Isoflurane inhibition of endocytosis is an anesthetic mechanism of action. Curr Biol 2022; 32: 3016–3032 e3 [PubMed: 35688155]
22. Zhou JX, Liu J: The effect of temperature on solubility of volatile anesthetics in human tissues. Anesth Analg 2001; 93: 234–8 [PubMed: 11429373]
23. Chartrand R: Numerical Differentiation of Noisy, Nonsmooth Data. ISRN Applied Mathematics 2011; 2011: 1–11
24. Fano RM: Transmission of Information: A Statistical Theory of Communications. American Journal of Physics 1961; 29: 793–794
25. Ting HK: On the Amount of Information. Theory of Probability & Its Applications 1962; 7: 439–447
26. Otsu N: A threshold selection method from gray-level histograms. IEEE Transactions on Systems, Man, and Cybernetics 1979; 9: 62–66
27. Liao P-S, Chen T-S, Chung P-C: A fast algorithm for multilevel thresholding. J. Inf. Sci. Eng 2001; 17: 713–727
28. Hudson AE: Anesthesia as Decoupling? Anesthesiology 2020; 133: 11–12 [PubMed: 32472806]

29. Cook SJ, Jarrell TA, Brittin CA, Wang Y, Bloniarz AE, Yakovlev MA, Nguyen KCQ, Tang LT, Bayer EA, Duerr JS, Bulow HE, Hobert O, Hall DH, Emmons SW: Whole-animal connectomes of both Caenorhabditis elegans sexes. Nature 2019; 571: 63–71 [PubMed: 31270481]
30. Gendrel M, Atlas EG, Hobert O: A cellular and regulatory map of the GABAergic nervous system of C. elegans. Elife 2016; 5
31. Pereira L, Kratsios P, Serrano-Saiz E, Sheftel H, Mayo AE, Hall DH, White JG, LeBoeuf B, Garcia LR, Alon U, Hobert O: A cellular and regulatory map of the cholinergic nervous system of C. elegans. Elife 2015; 4
32. Serrano-Saiz E, Poole RJ, Felton T, Zhang F, De La Cruz ED, Hobert O: Modular control of glutamatergic neuronal identity in C. elegans by distinct homeodomain proteins. Cell 2013; 155: 659–73 [PubMed: 24243022]
33. Yemini E, Lin A, Nejatbakhsh A, Varol E, Sun R, Mena GE, Samuel ADT, Paninski L, Venkatachalam V, Hobert O: NeuroPAL: A Multicolor Atlas for Whole-Brain Neuronal Identification in C. elegans. Cell 2021; 184: 272–288.e11 [PubMed: 33378642]
34. Nichols ALA, Eichler T, Latham R, Zimmer M: A global brain state underlies C. elegans sleep behavior. Science 2017; 356
35. Blain-Moraes S, Tarnal V, Vanini G, Bel-Behar T, Janke E, Picton P, Golmirzaie G, Palanca BJA, Avidan MS, Kelz MB, Mashour GA: Network Efficiency and Posterior Alpha Patterns Are Markers of Recovery from General Anesthesia: A High-Density Electroencephalography Study in Healthy Volunteers. Frontiers in Human Neuroscience 2017; 11
36. Hashmi JA, Loggia ML, Khan S, Gao L, Kim J, Napadow V, Brown EN, Akeju O: Dexmedetomidine Disrupts the Local and Global Efficiencies of Large-scale Brain Networks. Anesthesiology 2017; 126: 419–430 [PubMed: 28092321]
37. Lee U, Ku S, Noh G, Baek S, Choi B, Mashour GA: Disruption of Frontal-Parietal Communication by Ketamine, Propofol, and Sevoflurane. Anesthesiology 2013; 118: 1264–1275 [PubMed: 23695090]
38. Liang Z, King J, Zhang N: Intrinsic Organization of the Anesthetized Brain. The Journal of Neuroscience 2012; 32: 10183–10191 [PubMed: 22836253]
39. Clement EA, Richard A, Thwaites M, Ailon J, Peters S, Dickson CT: Cyclic and Sleep-Like Spontaneous Alternations of Brain State Under Urethane Anaesthesia. PLoS ONE 2008; 3: e2004 [PubMed: 18414674]
40. Hudson AE, Calderon DP, Pfaff DW, Proekt A: Recovery of consciousness is mediated by a network of discrete metastable activity states. Proceedings of the National Academy of Sciences 2014; 111: 9283–9288
41. Ishizawa Y, Ahmed OJ, Patel SR, Gale JT, Sierra-Mercado D, Brown EN, Eskandar EN: Dynamics of Propofol-Induced Loss of Consciousness Across Primate Neocortex. The Journal of Neuroscience 2016; 36: 7718–7726 [PubMed: 27445148]
42. Kato S, Kaplan HS, Schrodel T, Skora S, Lindsay TH, Yemini E, Lockery S, Zimmer M: Global brain dynamics embed the motor command sequence of Caenorhabditis elegans. Cell 2015; 163: 656–69 [PubMed: 26478179]
43. Proekt A, Hudson AE: A stochastic basis for neural inertia in emergence from general anaesthesia. BJA: British Journal of Anaesthesia 2018; 121: 86–94 [PubMed: 29935600]
44. Connor CW: A Forensic Disassembly of the BIS Monitor. Anesth Analg 2020; 131: 1923–1933 [PubMed: 33093360]
45. Connor CW: Open Reimplementation of the BIS Algorithms for Depth of Anesthesia. Anesth Analg 2022; 135: 855–864 [PubMed: 35767469]

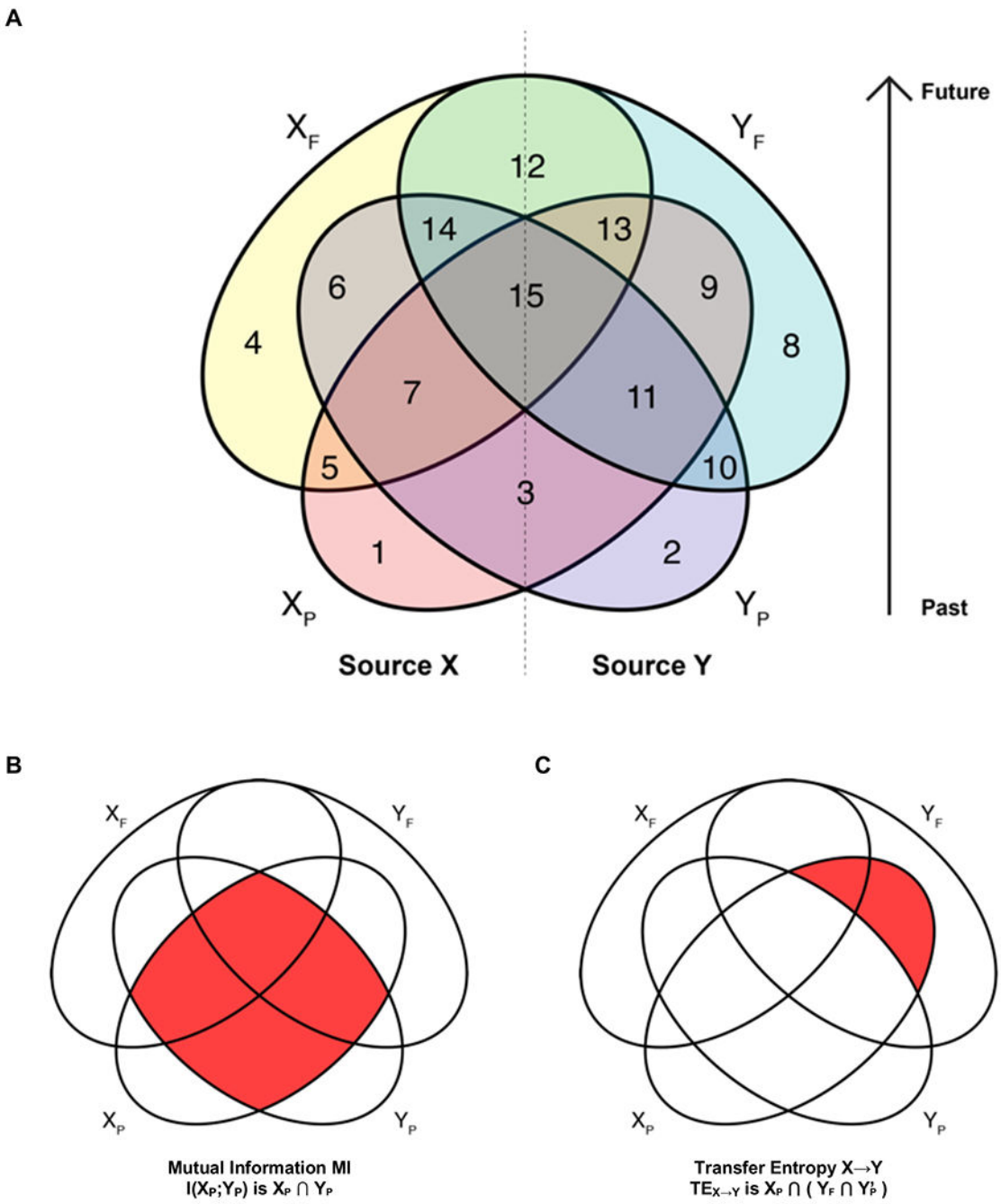

Figure 1.

A four-signal model for entropy-based information transfer between neuronal pairs.

A) Venn diagram of the four-signal model of past and future information content of two sources X and Y. The 15 regions are numbered by binary combination of $\mathbf{X_P}$, $\mathbf{Y_P}$, $\mathbf{X_F}$ and $\mathbf{Y_F}$ with values of 1, 2, 4 and 8 respectively. The region colors are assigned according to shading combinations of the base colors shown in regions 1, 2, 4 and 8.

B) The entropy quantity of Mutual Information (MI), representing the information that is common between the past states of source X and Y. Graphically, this corresponds to the

intersection of the regions $\mathbf{X_P}$ and $\mathbf{Y_P}$, i.e. the combination of regions 3, 7, 11, 15, described in set notation as $\mathbf{X_P} \cap \mathbf{Y_P}$, whose information content is therefore $H(X_P) + H(Y_P) - H(X_P, Y_P)$. C) The entropy quantity of Transfer Entropy from X to Y ($TE_{X \to Y}$), representing the information that is present in the future state of Y (Y_F) that can be predicted from the past of X (X_P) but not the past of Y (Y_P), and therefore represents causal transmission of information from X to Y. Graphically, this corresponds to the intersection of regions $\mathbf{X_P}$ and $\mathbf{Y_F}$ but not $\mathbf{Y_P}$, i.e. the combination of regions 9 and 13 described in set notation as $\mathbf{X_P} \cap (\mathbf{Y_F} \cap \mathbf{Y_P'})$, whose information content is therefore $H(X_P, Y_P) + H(Y_P, Y_F) - H(X_P, Y_P, Y_F) - H(Y_P)$.

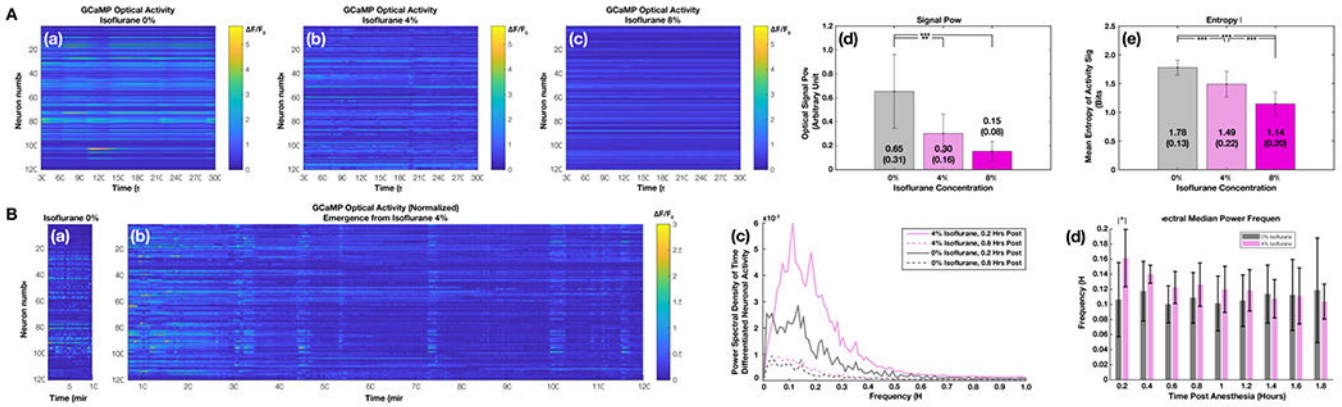

Figure 2.

Isoflurane exposure suppresses power and Shannon entropy of neuronal activity signals, and early emergence from isoflurane exposure is characterized by a quickly resolving high-frequency spectral shift.

Aabc) Fluorescent optical activity of 120 neurons in the head of C. *elegans* equilibrated to atmospheres of 0%, 4% and 8% isoflurane respectively. Color represents normalized GCaMP6s fluorescence activity in a cytoplasmic shell surrounding each tracked neuronal nucleus.

Ad) Decreasing total signal power under increasing concentrations of isoflurane. Mean signal power ± SD of neuronal activity traces recorded from animals equilibrated to room air, 4% or 8% isoflurane.

Ae) Mean Shannon entropy ± SD of quantized neuronal activity traces recorded from animals equilibrated to room air, 4% or 8% isoflurane.

Bab) Intensity traces of neuronal activity in 120 neurons in the *C. elegans* head ganglia before isoflurane exposure and as the animal emerges from equilibration to 4% isoflurane over 120 minutes.

Bc) Mean power spectral density of the time-differentiated neuronal activity traces 0.2 and 0.8-hours post-exposure to either room air or 4% isoflurane.

Bd) Mean spectral median power frequency (MPF) ± SD of neuronal traces in animals equilibrated to room air or 4% isoflurane, calculated at 12-minute epochs post-exposure. Error bars show the standard error of the mean. (* $P < 0.05$, ** $P < 0.01$, *** $P < 0.001$)

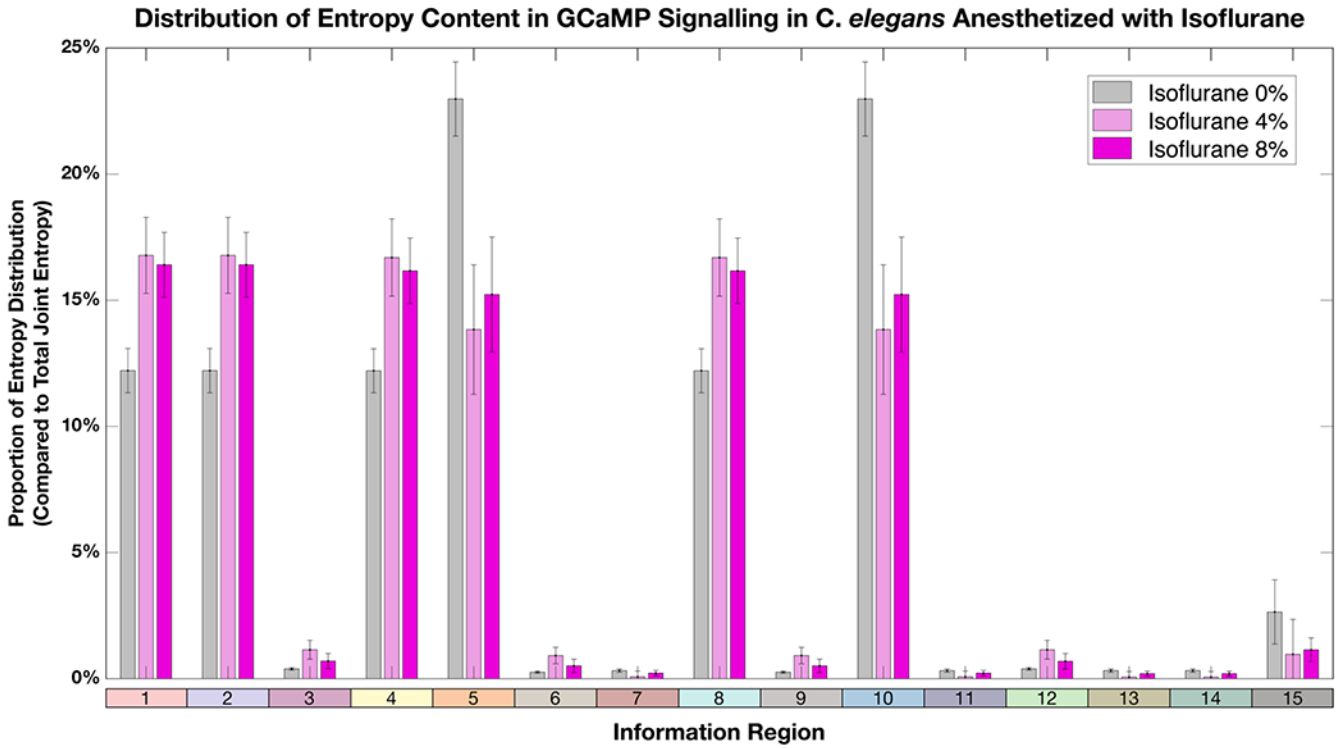

Figure 3.

Exposure to isoflurane significantly alters the distribution of entropy within the 4-signal information transfer model. Mean entropy content ± SD in information regions 1-15 of the 4-signal information transfer model in animals exposed to room air, 4%, or 8% isoflurane (n=10). Entropy content was calculated for each neuron pair recorded in each animal (14400 neuron pairs/animal/exposure condition), normalized to the total joint entropy of the 4-signal model, and then averaged by exposure condition. Error bars show the standard error of the mean.

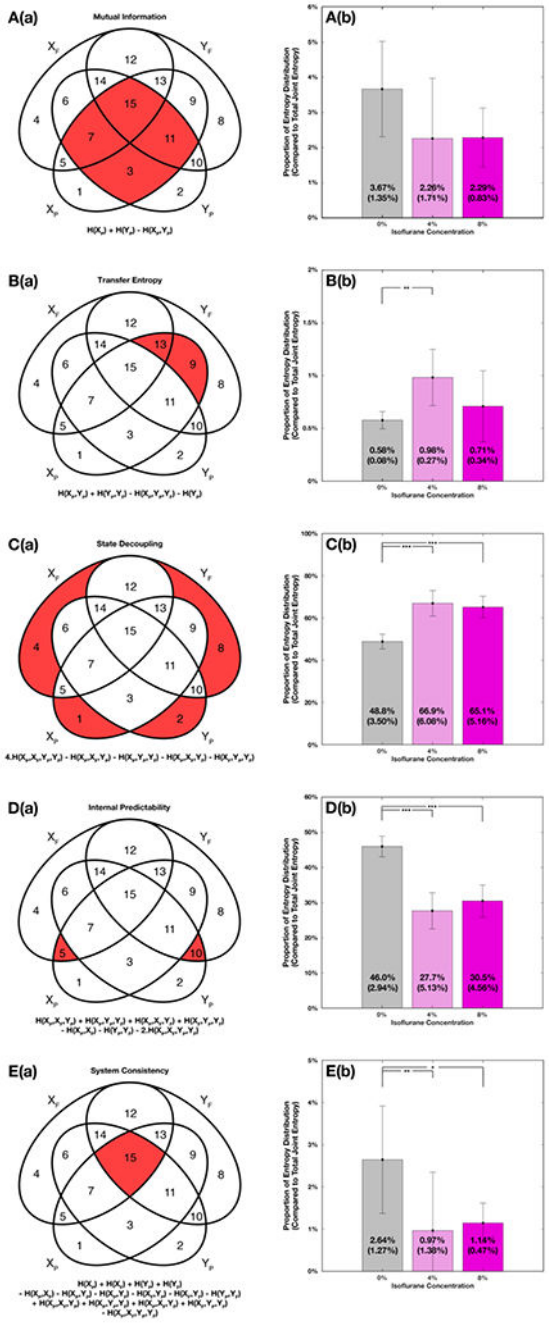

Figure 4.

The anesthetized state can be characterized by shifts in novel entropy-based measures of information transfer between neuron pairs.

Aa-Ea) Selected information region clusters in the 4-signal model representative of information theoretic metrics: Mutual Information, Transfer Entropy, State Decoupling, Internal Predictability, and System Consistency. Colored Venn areas represent the combined information regions that compose each metric. The equations used to calculate each metric from joint entropies are also shown.

Ab-Eb) Mean proportional entropy content ± SD in the selected information region clusters in neuronal activity trace pairs recorded from animals exposed to room air, 4% and 8% isoflurane.

Error bars show the standard error of the mean. (* $P < 0.05$, ** $P < 0.01$, *** $P < 0.001$)

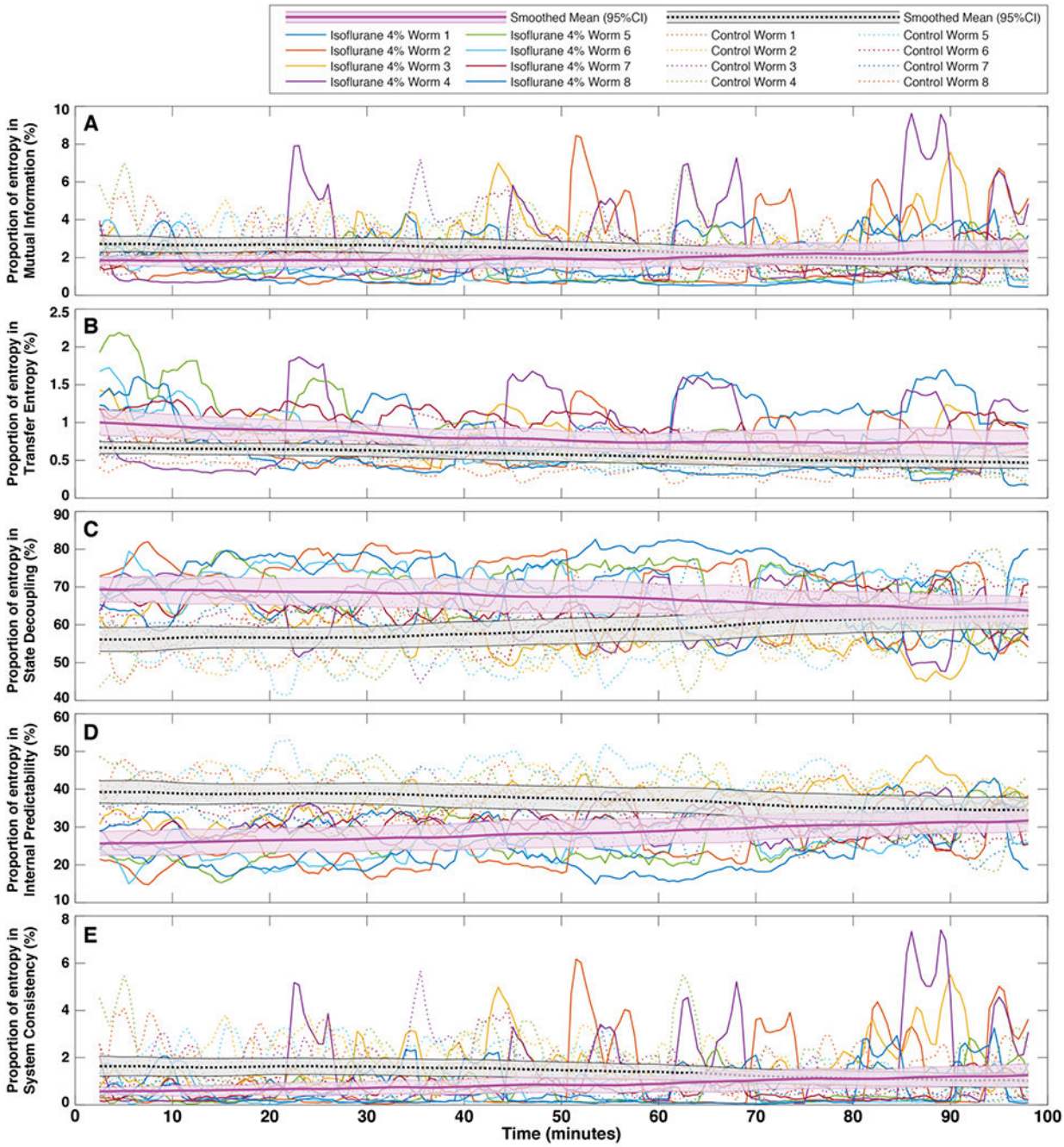

Figure 5.

Alterations in entropy-based measures of neuronal-pair information transfer resolve to baseline levels non-linearly as animals emerge from isoflurane anesthesia: respectively Mutual Information, Transfer Entropy, State Decoupling, Internal Predictability, and System Consistency.

A-E) Time-smoothed means ± 95% CI of proportional entropy content in information region clusters corresponding to measures of information transfer in animals emerging from anesthesia with isoflurane 4% and in room-air exposed controls. Metrics as calculated for

individual animals are also shown for each measurement type. (n=8 isoflurane exposed, n=8 controls).

Table 1

Conversion table from combinations of information regions, as enumerated in Figure 1A, into combinations of entropy measures H derived from the past and future states of sources X and Y. This table allows the graphical representation of information, as shown in Figure 1 and Figure 4, to be converted into simple additive combinations of elementary entropy functions. Rows are colored according to the schema used in Figure 1A.

		ENTROPY MEASURE														
		$H(X_P)$	$H(Y_P)$	$H(X_F)$	$H(Y_F)$	$H(X_P, Y_P)$	$H(X_P, X_F)$	$H(X_P, Y_F)$	$H(Y_P, X_F)$	$H(Y_P, Y_F)$	$H(X_F, Y_F)$	$H(X_P, Y_P, X_F)$	$H(X_P, Y_P, Y_F)$	$H(X_P, X_F, Y_F)$	$H(Y_P, X_F, Y_F)$	$H(X_P, Y_P, X_F, Y_F)$
INFORMATION REGION	1	0	0	0	0	0	0	0	0	0	0	0	0	0	−1	1
	2	0	0	0	0	0	0	0	0	0	0	0	0	−1	0	1
	3	0	0	0	0	0	0	0	0	0	−1	0	0	1	1	−1
	4	0	0	0	0	0	0	0	0	0	0	0	−1	0	0	1
	5	0	0	0	0	0	0	0	0	−1	0	0	1	0	1	−1
	6	0	0	0	0	0	0	−1	0	0	0	0	1	1	0	−1
	7	0	0	0	−1	0	0	1	0	1	1	0	−1	−1	−1	1
	8	0	0	0	0	0	0	0	0	0	0	−1	0	0	0	1
	9	0	0	0	0	0	0	0	−1	0	0	1	0	0	1	−1
	10	0	0	0	0	0	−1	0	0	0	0	1	0	1	0	−1
	11	0	0	−1	0	0	1	0	1	0	1	−1	0	−1	−1	1
	12	0	0	0	0	−1	0	0	0	0	0	1	1	0	0	−1
	13	0	−1	0	0	1	0	0	1	1	0	−1	−1	0	−1	1
	14	−1	0	0	0	1	1	1	0	0	0	−1	−1	−1	0	1
	15	1	1	1	1	−1	−1	−1	−1	−1	−1	1	1	1	1	−1